Environ. Sci. Technol. **2010,** *44,* 9225–9232

Potential Impacts of Leakage from Deep CO_2 Geosequestration on Overlying Freshwater Aquifers

MARK G. LITTLE*,† AND ROBERT B. JACKSON†,‡

Center on Global Change, Duke University, Durham, North Carolina 27708, United States, and Nicholas School of the Environment and Biology Department, Duke University, Durham, North Carolina 27708-0338, United States

Received July 20, 2010. Revised manuscript received October 12, 2010. Accepted October 13, 2010.

Carbon Capture and Storage may use deep saline aquifers for CO_2 sequestration, but small CO_2 leakage could pose a risk to overlying fresh groundwater. We performed laboratory incubations of CO_2 infiltration under oxidizing conditions for >300 days on samples from four freshwater aquifers to 1) understand how CO_2 leakage affects freshwater quality; 2) develop selection criteria for deep sequestration sites based on inorganic metal contamination caused by CO_2 leaks to shallow aquifers; and 3) identify geochemical signatures for early detection criteria. After exposure to CO_2, water pH declines of 1−2 units were apparent in all aquifer samples. CO_2 caused concentrations of the alkali and alkaline earths and manganese, cobalt, nickel, and iron to increase by more than 2 orders of magnitude. Potentially dangerous uranium and barium increased throughout the entire experiment in some samples. Solid-phase metal mobility, carbonate buffering capacity, and redox state in the shallow overlying aquifers influence the impact of CO_2 leakage and should be considered when selecting deep geosequestration sites. Manganese, iron, calcium, and pH could be used as geochemical markers of a CO_2 leak, as their concentrations increase within 2 weeks of exposure to CO_2.

Introduction

Carbon Capture and Storage (CCS) represents a suite of technologies developed to separate, compress, transport, and sequester securely underground the CO_2 produced from power plants and other industrial facilities. Currently, power plant flue gases containing CO_2 are released directly to the atmosphere where they contribute to the steady rise in atmospheric CO_2 and climate change (*1, 2*). However, a full understanding of long-term environmental risks is needed before large-scale CCS implementation is feasible (*3*−*5*).

The engineering requirements and potential environmental impact of CCS technologies are currently being investigated in many locations around the world, including the Sleipner field in the North Sea (*6*), offshore Japan (*7*), and Otway, Australia (*8*). In the U.S., the Department of Energy has initiated seven regional CCS projects in collaboration with industry and academia under the Regional Carbon Sequestration Partnership (*9*). The potential risk of CO_2 leakage has already contributed to local opposition to CCS implementation (*10*−*12*). On time scales appropriate for geosequestration (>1000 yrs), the bulk of CO_2 sequestered in a properly chosen saline aquifer is unlikely to escape because of solubility trapping (*13, 14*). However, given the heterogeneous nature of the subsurface, minor CO_2 leakage along faults, old petroleum wells, or other pathways will persist and will be thermodynamically difficult to seal completely by precipitation of carbonate minerals (*10, 11, 15*−*17*). Standards for "acceptable" levels of leakage could translate into tons of CO_2 annually released from the deep storage aquifer into intermediate and shallow strata (*18*). Because freshwater aquifers used for drinking water, industry, and agriculture lie directly above possible geosequestration locations, leaks could form carbonic acid in groundwater resources before surface leakage of CO_2 were detected (e.g., refs *10*, *19*, and *20*).

Although increases in carbonic acid may be buffered by carbonate dissolution, a lowering of aquifer water pH may release harmful metals, such as arsenic and uranium, into the water (*21*−*23*). Such impacts on shallow aquifer composition have been investigated previously in field injection studies (*23, 24*), model simulations (*25, 26*), and short-term batch-reaction experiments (*27*). Our study focuses on the long-term impacts of CO_2 leakage on four relatively shallow aquifer systems overlying possible deep saline geosequestration sites: Aquia and Virginia Beach in the Virginia and Maryland tidewater region; Mahomet in Illinois; and Ogallala in southern high plains of Texas. We performed laboratory incubations under oxidizing conditions for more than 300 days to 1) understand how CO_2 leaks from deep geosequestration may affect water quality in overlying shallow drinking-water aquifers; 2) develop selection criteria for sequestration sites based on inorganic metal contamination caused by CO_2 leaks; and 3) identify geochemical signatures in affected waters which could be used as early detection criteria.

Methods

Sample Selection. We identified freshwater aquifers that overlie potential deep saline geosequestration target units (*13*−*15, 28*). To prioritize the potential risks, samples were collected only from those drinking-water aquifers where natural, in situ concentrations of As, U, Ra, Cd, Cr, Cu, Pb, Hg, or Se were greater than 10% of U.S. Environmental Protection Agency's primary maximum contaminant level (MCL) for drinking water (*29, 30*). Noncontaminated groundwater concentrations greater than 10% were interpreted as a qualitative indication of the presence of these metals in solid phase in the aquifer sediment. Approximately 1 kg of dry aquifer sediment from 17 distinct locations within the Aquia (MD), Virginia Beach (VA), Mahomet (IL), and Ogallala (TX) aquifers was acquired from the Illinois State Geological Survey, the United States Geological Survey, the Virginia Department of Environmental Quality, and the Maryland Geological Survey (Table 1, Figure 1).

Laboratory Incubations. All aquifer sediment samples were oven-dried for 36 h at 110 °C in order to minimize microbial activity over the long-duration (>300 days) experiment. Dry samples were divided as follows: two ∼400 g subsamples were set aside for the groundwater experiment; one ∼5 g aliquot was powdered on a stainless steel mill for mass spectrometry; and ∼1 g was epoxy mounted for microprobe analysis, the latter performed on 6 samples. Methods for the preparations of rock powders for whole-

* Corresponding author phone: (919)681-7180; fax: (919)660-7425; e-mail: 6r4h@post.harvard.edu.
† Center on Global Change.
‡ Nicholas School of the Environment and Biology Department.

10.1021/es102235w
Published on Web 10/26/2010

TABLE 1. Sample Locations and Descriptions

sample name	avg depth (m)	well name	aquifer reached	sample description
AQ1	14.8	AA De 100	Aquia	very fine sand
VB1	13	Old Pungo Ferry Road (62A-21) USGS# 363714076063501	Virginia Beach	medium quartz sand with trace black grains[a]
VB2	11	Creeds Elementary (62B-15) USGS# 363812076021202	Yorktown Confining Unit	medium quartz sand with chalcopyrite[a]
VB3	5	Oceana II (62C-31) USGS# 365046076041601	Virginia Beach	medium quartz sand with unidentified black grains[a]
VB4	19.4	Bonney Bright North (63A-1) USGS# 363337075595001	Yorktown-Eastover	coarse quartz sand shells[a]
VB5	36.1	Beach Gardens Park (63C-30) USGS# 365124075590701	Yorktown-Eastover	coarse quartz sand shells[a]
MH1	84.7	PIAT 08 03A	Mahomet	sand, primarily Na/K feldspars, quartz, dolomite, and Fe oxides with Ti-oxide present, trace As[b]
MH2	78	CHAM 07 01A		
MH3	92.2	CHAM 08 09A		
MH4	79.1	CHAM 09 03A		
OG1	8.4	MWR-B	Ogallala	fine sand, primarily quartz and K/Na feldspars, Fe- and Ti-oxides, coarse calcite grains present[b,c]
OG2	9.9	USGS# 335830102444201		
OG3	12.3	MAPLE (MPL)		fine sand, primarily quartz, calcite, Ca/K feldspars, and unidentified alumino-silicates present, trace Fe/Ti oxides[b,c]
OG4	19.4			
OG5	29.1	USGS# 33495102545001		
OG6	41.6			
OG7	21.1	JWR		fine sand, primarily quartz, K/Na/Ca feldspars, Fe oxide, calcite present, trace Ti oxide[a,c]
OG8	36.1			
OG9 *	45.3	USGS# 334043102365501		
OG10	48.3			

[a] Sample description from refs *32* and *33*. [b] Qualitative microprobe data included in the sample description. [c] Additional sample description from ref *45*.

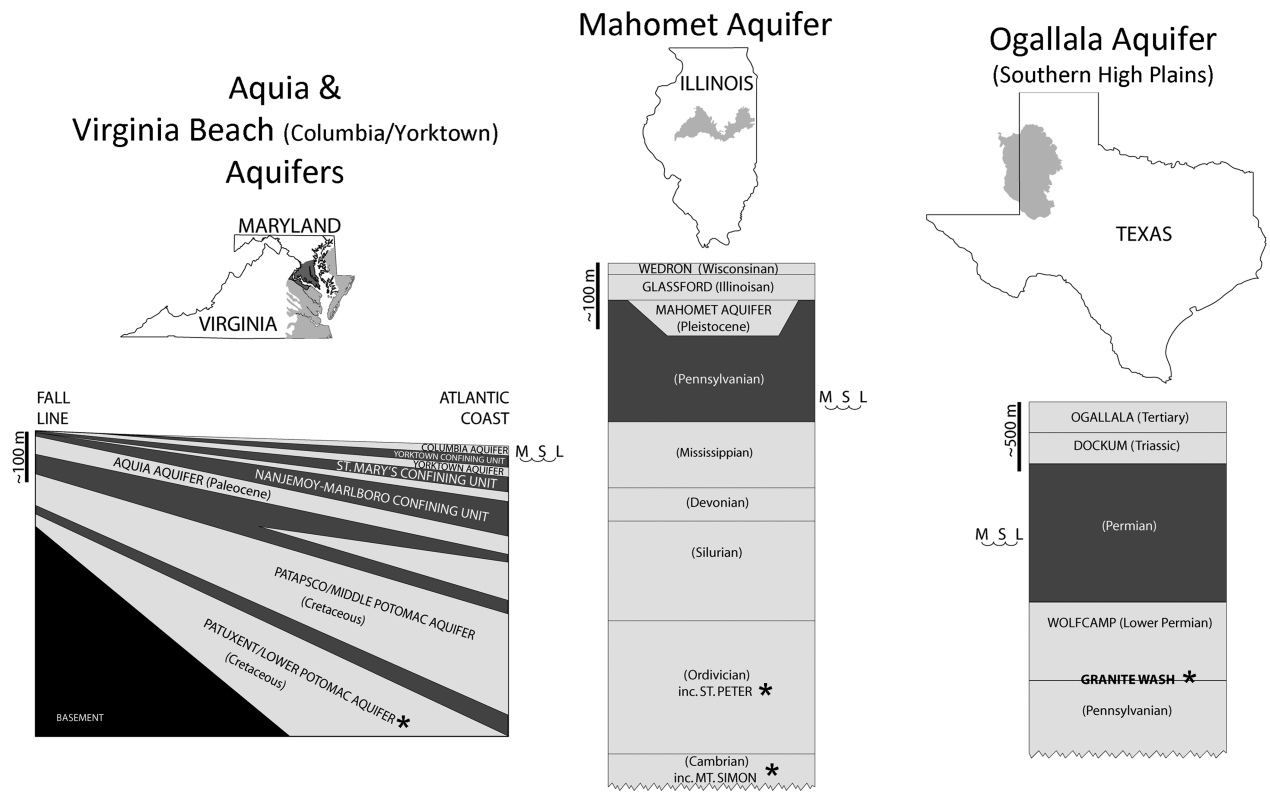

FIGURE 1. Areal map and vertical cross sections of central Illinois, the Texas panhandle, and Virginia and Maryland tidewater region. Confining units are shown in dark gray. Sediment samples are from the Aquia (MD), Virginia Beach (Columbia/Yorktown) (VA), Mahomet (IL), and Ogallala (TX) aquifers. Possible CO_2 sequestration strata indicated with asterisks (*37*–*44*).

rock acid digestion and subsequent fluid analysis were adapted from ref *31* and performed on each of the 17 samples.

The 17 pairs of 400-g samples were weighed precisely and placed into bottles with 18.6 MΩ/cm nanopure makeup water at a water-to-rock ratio of 3 to 1, were maintained at approximately 20 °C, and are hereafter referred to as the *groundwater experiment*. One set of 17 bottles was sealed and placed in an opaque box to serve as the control, and the

TABLE 2. Average Water pH and Alkali and Alkaline Earth Element Concentrations of the Groundwater Experiment, $+CO_2$, and Control Values[a]

	pH		Li, ppb		Mg, ppm		Ca, ppm		Rb, ppb		Sr, ppb	
MCL	6.5−8.5											
	$+CO_2$	ctrl	$+CO_2$	ctrl	$+CO_2$	ctrl	$+CO_2$	ctrl	$+CO_2$	ctrl	$+CO_2$	ctrl
AQ1	4.47	5.79	6.6	2.7	3.4	0.27	6.2	0.5	10.2	3.2	29	1.6
VB1	4.22	4.24	25	21	12	14	8.2	7.4	1.3	1.2	113	116
VB2	4.26	5.27	2.5	0.12	2.5	0.08	5.9	0.4	2.0	0.40	175	5.1
VB3	3.11	3.12	72	73	14	16	26	18	11	9	54	35
VB4	5.18	6.17	35	22	17	23	103	106	3.3	3.2	450	381
VB5	5.73	6.72	79	53	19	24	517	501	8.0	8	4230	4243
MH1	5.64	7.41	13	2.2	15	3.6	276	18	2.4	1.1	630	82
MH2	5.64	7.36	15	7.2	14	3.0	288	18	3.3	1.7	911	124
MH3	5.63	7.56	13	4.5	14	2.4	302	12	3.0	1.2	642	63
MH4	5.85	6.89	16	12	16	17	239	88	2.6	2.4	596	277
OG2	5.65	7.21	94	41	16	6.5	275	20	2.2	1.2	1894	358
OG3	5.77	7.26	250	43	21	17	323	41	2.7	1.2	3971	1488
OG5	5.73	7.37	26	11	17	6.0	328	17	2.3	0.74	2856	377
OG6	5.80	6.84	45	17	16	7.8	273	16	2.4	0.73	3425	375
OG7	5.74	7.20	40	7.2	17	5.4	348	20	1.8	0.60	2064	358
OG8	5.69	7.36	38	16	16	11	279	23	1.7	0.92	2159	537
OG10	5.67	7.64	19	9.4	19	6.3	314	12	2.0	0.80	1938	306

[a] Data averaged over the final five sampling dates for the $+CO_2$ experiment: AQ on days 194, 244, 272, 305, and 334; VB on days 180, 230, 258, 291, and 320; MH and OG on days 204, 254, 282, 315, and 344. Data averaged over two sampling dates for the control (ctrl): AQ on days 194 and 305; VB on days 180 and 291; MH and OG on days 204 and 315. Averages do not include Mg data from AQ on day 194, VB on day 180, MH and OG on day 204. These days all correspond with sampling date 12/16/09 when drastic deviations in various element concentrations in both the $+CO_2$ and control experiments were observed.

other set of 17 bottles was prepared for exposure to CO_2, or "$+CO_2$", as follows. A stream of 99.8% pure CO_2 was piped at atmospheric pressure to each bottle through 17 individually flow-regulated channels at a constant flow rate of 0.2 L/min for 320 to 344 days. This flow rate is roughly equivalent to 0.005% of the CO_2 emissions at a typical 500 megawatt coal-fired power plant (*1*). Each channel is fed into the bottles through a 2-hole rubber stopper and delivers the CO_2 into the bottles via a plastic bubble diffuser that is completely inundated and ~1 cm above the surface of the aquifer sediment. The other hole in the stopper is connected to an exhaust tube leading from the headspace of each incubation bottle. Each bottle has an independent CO_2 delivery and exit system and is covered in aluminum foil to minimize photosynthesis.

At intervals of a week to a month (for a maximum of 344 days for the Mahomet and Ogallala samples, 320 days for Virginia Beach, and 334 days for Aquia), ~3 mL aliquots were removed from each bottle and tested for pH within 10 s to minimize the effect of degassing. A second aliquot was removed and forced through a syringe with 2-μm filter paper to produce 2 mL of filtered experimental groundwater from each bottle. The 2-mL aliquots were diluted to 10 mL with quartz distilled 18 MΩ/cm water for ICP-MS analysis. After each sampling, nanopure water was added to the bottles to maintain the 3:1 water-to-rock ratio. Sampling and evaporation accounted for water losses in the range of 5 to 20% for a 30-day sampling interval; thus the maximum effect of these losses is an artificial element concentration increase of 20%. Bottles were gently agitated for ~10 s after each sampling and at no other time during the experiment.

Inorganic elemental concentrations were determined by inductively coupled plasma mass spectrometry (ICP-MS) on a VG PlasmaQuad 3 at the Duke University Division of Earth and Ocean Sciences. For the whole-rock samples, Li, V, Cr, Co, Ni, Cu, Zn, Rb, Sr, Mo, Ba, and U were analyzed; for the experimental groundwater, Li, B, Mg, Al, Ca, V, Cr, Mn, Fe, Co, Ni, Cu, Zn, As, Se, Rb, Sr, Mo, Cd, Ba, and U were analyzed. Instrument calibration standards were prepared from serial dilutions of certified water standard NIST1643e. Samples and standards were diluted to the same proportions with an internal standard solution in 2% HNO_3 containing 10 parts per billion (ppb) In, Tm, and Bi to monitor and correct for instrument drift. All dilutions were carried out with solutions

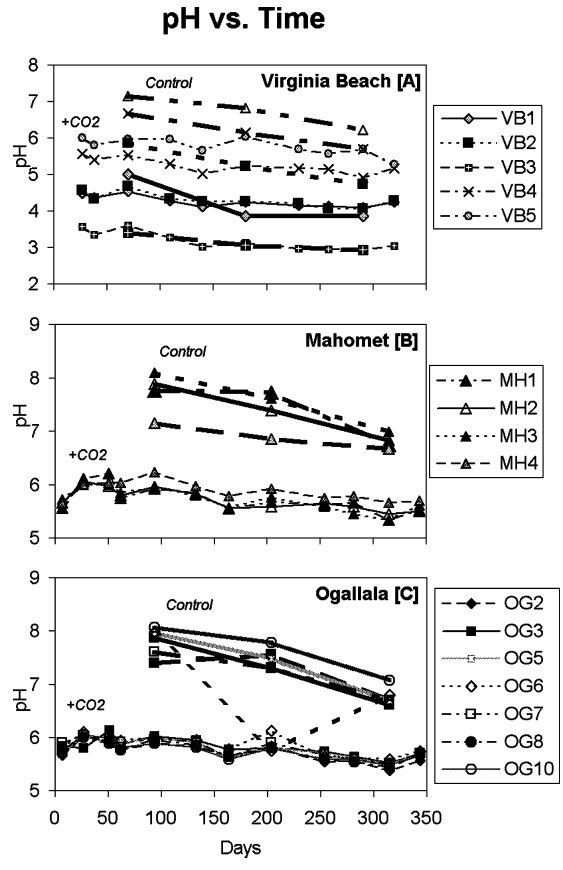

FIGURE 2. pH in groundwater experiments plotted against time. $+CO_2$ experiment data collection began on day ~10. Control experiment data collection began on day ~45.

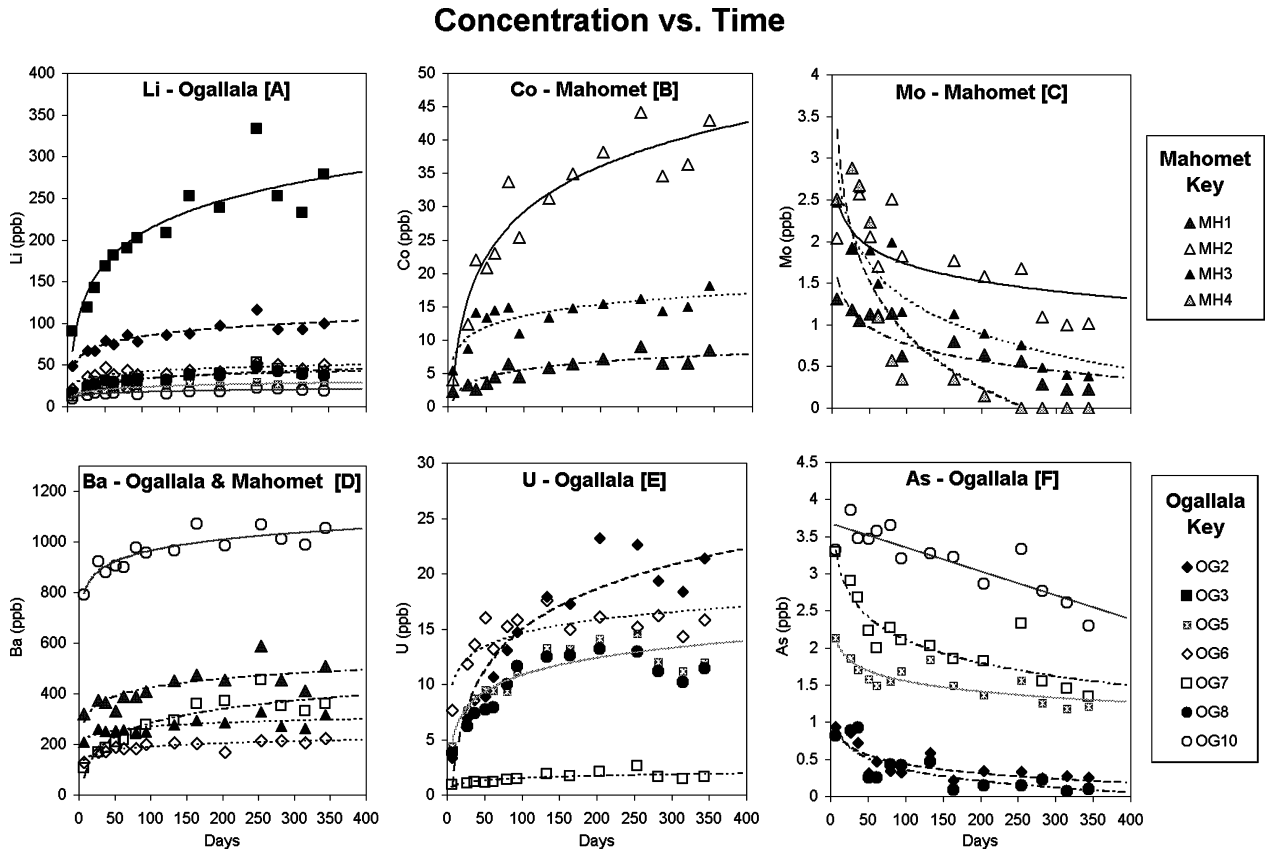

FIGURE 3. $+CO_2$ concentrations plotted against time and fit to log curves unless indicated as linear. [A] **Li: OG2 $R^2 = 0.84$; OG3 $R^2 = 0.84$; OG5 $R^2 = 0.90$; OG6 $R^2 = 0.72$; OG7 $R^2 = 0.85$; OG8 $R^2 = 0.86$; OG10 $R^2 = 0.63$.** [B] **Co: MH1 $R^2 = 0.78$; MH2 $R^2 = 0.90$; MH3 $R^2 = 0.71$.** [C] **Mo: MH1 $R^2 = 0.78$; MH2 $R^2 = 0.47$; MH3 $R^2 = 0.82$; MH4 $R^2 = 0.73$.** [D] **Ba: OG6 $R^2 = 0.76$; OG7 $R^2 = 0.86$; OG10 $R^2 = 0.80$; MH1 $R^2 = 0.61$; MH3 $R^2 = 0.62$.** [E] **U: OG2 $R^2 = 0.89$; OG5 $R^2 = 0.79$; OG6 $R^2 = 0.62$; OG7 $R^2 = 0.53$; OG8 $R^2 = 0.78$.** [F] **As: OG2 $R^2 = 0.72$; OG5 $R^2 = 0.73$; OG7 $R^2 = 0.83$; OG8 $R^2 = 0.68$; OG10 (linear) $R^2 = 0.75$.**

prepared from deionized-quartz-distilled H_2O and quartz-distilled HNO_3. Instrument drift was also monitored and corrected for each element analyzed by analysis of the calibration standards at regular intervals between analysis of samples and standards. To allow for determination of U and Th concentrations, NIST1643e was spiked with plasma-grade single-element solutions of U and Th prior to serial dilution. External precision for most elements is typically 4% or less, based on replicate analysis of samples and standards.

The microprobe analysis employed an energy dispersive spectrometry on a Cameca Camebax electron microprobe for a qualitative identification of mineral grain cross sections. The microprobe was operated at 15 kV accelerated potential and 15 μAmp beam current on polished samples. Data were reduced using 4Pi Revolution software.

Results

The chemical composition of our groundwater experiments was significantly affected by the addition of CO_2. All $+CO_2$ groundwater experiments produced a pH below EPA's minimum MCL of 6.5 units (Table 2, Figure 2). Most alkali and alkaline metal concentrations (Li, Mg, Ca, Rb, Sr) in the $+CO_2$ experiments were >30% higher than in the control (Table 2). For instance, Li shows a significant, time-dependent increasing trend (Figure 3a). Decreases of Mg concentrations in MH4, VB3, VB4, and VB5 and decreases of Ca in VB4 were the only exceptions to the enhanced dissolution of the earth metals in response to the addition of CO_2.

Concentrations of some transition metals, including Mn, Fe, Co, Ni, and Zn, were higher by more than 1000% in $+CO_2$ experiments relative to the control treatments across all aquifers (Table 3). In general, the high concentrations observed in the $+CO_2$ experiments were apparent within 2 weeks of exposure and did not continue to increase over the remainder of the experiment. However, Co in M1, M2, and M3 did exhibit a significant, logarithmic time-dependent increase over the entire experiment (Figure 3b). The remaining transition metals did not behave the same across all aquifers. Cd in the $+CO_2$ Aquia, Virginia Beach, and Mahomet experiments was higher than the control treatments by as much as 1000%. Yet, Cd in the $+CO_2$ Ogallala experiments produced lower or roughly equivalent concentrations than the control. Al, V, and Cr in $+CO_2$ Virginia Beach samples were elevated relative to the control; however, Al, V, and Cr in $+CO_2$ Aquia, Mahomet, and Ogallala experiments were lower relative to the control. Cu was generally higher in the Aquia and Ogallala $+CO_2$ experiments but lower in MH2, MH3, VB1, VB3, and OG2 $+CO_2$ experiments relative to the control treatments. $+CO_2$ Mo was lower than the control by 1 to 2 orders of magnitude in all aquifers and produced a significant, time-dependent logarithmic decrease in Mahomet samples (Figure 3c).

In response to exposure to CO_2, B, Ba, Tl, and U values were typically higher and As, Se, and Sb values were lower in the Aquia, Mahomet, and Ogallala samples relative to the control treatments (Figure 4, Table 4). Ba and U in some Ogallala and Mahomet $+CO_2$ experiments produced a significant, time-dependent logarithmic increase (Figure 3d,e), while As in some Ogallala $+CO_2$ experiments produced a time-dependent decrease (Figure 4f). In the Virginia Beach $+CO_2$ experiments, B and Ba were higher than in the control while As was lower relative to the control. Se, Sb, Tl, and U increased in some $+CO_2$ VB samples and decreased in others relative to the control (Table 4).

TABLE 3. Average Transition Metal Element Concentrations of the Groundwater Experiment, $+CO_2$, and Control Values[a]

	Al, ppb		V, ppb		Cr, ppb		Mn, ppb		Fe, ppb		Co, ppb		Ni, ppb		Cu, ppb		Zn, ppb		Mo, ppb		Cd, ppb	
MCL	50				100		50		300						1300		5000				5	
	$+CO_2$	ctrl	$+CO_2$	ctrl	$+CO_2$	ctrl	$+CO_2$	ctrl	$+CO_2$	ctrl	$+CO_2$	ctrl	$+CO_2$	ctrl	$+CO_2$	ctrl	$+CO_2$	ctrl	$+CO_2$	ctrl	$+CO_2$	ctrl
AQ1	5.6	29.6	0.13	0.44	0.13	2.8	109	3.9	9	63	0.73	0.03	4.6	0.16	1.84	0.12	25	36	0.13	0.06	3.0	0.12
VB1	106	162	2.0	1.5	6.1	4.4	354	393	1163	224	69	4.0	24	7.6	3.2	1.7	1299	118	0.15	0.13	0.57	0.37
VB2	108	1.4	0.06	0.13	0.21	0.08	553	63	3.6		3.7		2.8	0.05	0.47	0.13	736	28	0.13	0.02	0.67	
VB3	5341	5887	1.6	0.11	16	18	611	799	4729	188	789	953	1862	2135	11.0	27	2432	1631	0.13	0.05	2.8	3.3
VB4	11.1	3.6	0.20	0.15	0.31	0.23	1723	1139	3598	187	11	2.2	18	4.4	0.66	0.9	163	42	0.54	1.6	0.11	0.04
VB5	3.7	1.8	1.6	0.66	2.3	1.1	431	20	4604	1055	4.1	0.9	24	10	1.9	2.4	53	22	23	94	0.70	0.13
MH1	2.1	45	0.14	0.54	0.41	1.17	616	12	458	30	6.8	0.03	25	0.42	2.6	1.8	69	111	0.62	31	0.18	0.03
MH2	1.6	7.0	0.16	0.35	0.42	0.23	495	62	471	29	36	0.15	80	0.82	2.2	3.7	123	32	1.5	16	0.57	0.01
MH3	2.1	29	0.28	4.3	0.41	2.5	503	5.0	517	13	15	0.16	27	0.9	1.05	2.5	117	72	0.9	37	0.25	0.03
MH4	0.8	2.2	0.05	0.05	0.46	0.32	511	240	384	170	7.2	0.25	27	1.8	1.20	0.51	15	43	0.22	0.07	0.13	
OG2	2.6	3.7	1.9	70	1.0	1.2	552	2.6	481	29	12	0.06	171	1.4	13	15	26	7	20	66.95	0.07	0.07
OG3	21	2.3	3.9	91	1.0	0.69	36	0.2	577	64	1.4	0.06	14	0.7	1.3	0.42	12	32	89	79.95	0.10	0.08
OG5	6.8	6.8	8.8	14	1.8	4.0	461	0.3	558	26	1.7	0.02	35	0.33	2.2	0.44	129	34	3.2	48.10	0.03	0.04
OG6	2.8	6.2	17	31	7.2	5.0	444	0.4	468	22	0.46	0.04	11	0.29	1.5	0.38	87	102	2.1	57.68	0.02	0.06
OG7	3.5	11	7.9	78	0.46	0.55	214	3.9	652	30	1.3	0.08	7.8	0.42	1.7	0.91	15	76	4.8	16.92	0.01	0.01
OG8	1.6	5.4	0.34	36	0.83	4.7	694	10	1889	36	20	0.12	215	0.8	1.30	2.0	69	46	13	63.13	0.05	0.05
OG10	3.4	6.8	14	40	1.0	3.0	470	0.4	516	21	2.5	0.03	58	0.57	2.9	0.80	214	30	7.7	74.63	0.05	0.07

[a] Data averaged over the final five sampling dates for the $+CO_2$ experiment: AQ on days 194, 244, 272, 305, and 334; VB on days 180, 230, 258, 291, and 320; MH and OG on days 204, 254, 282, 315, and 344. Data averaged over two sampling dates for the control (ctrl): AQ on days 194 and 305; VB on days 180 and 291; MH and OG on days 204 and 315. Averages do not include Al data from AQ on day 194, VB on day 180, MH and OG on day 204.

FIGURE 4. Co vs Ni in $+CO_2$ Virginia Beach and Mahomet experiments. VB1 $R^2 = 0.95$; VB4 $R^2 = 0.98$; VB5 $R^2 = 0.74$; MH1 $R^2 = 0.93$; MH2 $R^2 = 0.98$; MH3 $R^2 = 0.61$; MH4 $R^2 = 0.83$.

Concentrations that exceeded their primary or secondary U.S. EPA MCL health standard and concentrations that exhibited a significant, time-dependent increase were of concern because the ultimate long-term equilibrium concentration may exceed the MCL (*29*). Mn and Fe exceeded the MCL in most samples, while Al exceeded its MCL only in VB1, VB2, and VB3. Zn concentrations in VB3 reached ~50% of the secondary MCL (2500 ppb) and Cd concentrations in VB3 and AQ1 exceeded 50% of the primary MCL (>2.5 ppb), but neither element exhibited a significant, long-term increasing trend. Cr and Cu concentrations were ~3 orders below MCL in all samples. Although As concentrations in some control Ogallala experiments exceeded the 10 ppb MCL, consistent with natural field measurements (*34*), the addition of CO_2 caused a decrease in As concentrations (Figure 3f). In some Ogallala and Mahomet samples, Ba displayed a significant, time-dependent increase, reaching 25 to 50% of the MCL (Figure 3d). Se, Sb, and Tl did not show a significant increasing trend; however, Se = 22 ppb in VB3 (selenium MCL = 50 ppb) and T*l* > 0.15 ppb in VB3, MH2, and MH4 (thallium MCL = 0.5 ppb). In both $+CO_2$ and control VB5 experiments, U exceeded the 30 ppb MCL. Uranium in the $+CO_2$ OG3 experiment also exceeded the MCL, and other Ogallala samples exhibited a time-dependent increasing trend without exceeding the MCL (Figure 3e). The continued time-dependent increase of Ba and U over >300 days of exposure to CO_2 justifies the need for even longer laboratory experiments and monitoring.

The carbonate-poor experiment samples (AQ1, VB1, VB2, VB3, and VB4) produced the lowest pH values and the lowest Ca concentrations among $+CO_2$ and control experiments (Tables 2 and 3). The low pH/low Ca composition may have resulted from mixing of nanopure water with carbonate-poor sediment and, in the case of the Virginia Beach samples which contain chalcopyrite, from the formation of sulfuric acid (*32, 33*). These samples, and particularly VB3, also produced the highest concentrations of Al, Cr, Co, Ni, Zn, Cd, As, and Se.

Discussion

Chemical detection of leakage into shallow aquifers from a deep CO_2 geosequestration site will be an integral part of a safe CCS system. CO_2 that infiltrates an unconfined freshwater

TABLE 4. Average Half-Metal and Other Measured Element Concentrations of the Groundwater Experiment, $+CO_2$, and Control Values[a]

	B, ppb		As, ppb		Se, ppb		Ba, ppb		Tl, ppb		U, ppb	
MCL			10		50		2000		0.5		30	
	$+CO_2$	ctrl	$+CO_2$	ctrl	$+CO_2$	ctrl	$+CO_2$	ctrl	$+CO_2$	ctrl	$+CO_2$	ctrl
AQ1	55	64	0.04	0.04	0.49	2.2	25	1.5	0.007	0.000	0.03	
VB1	361	80	0.81	0.39	1.5	1.4	20	16	0.012	0.012	0.13	0.10
VB2	27	17	0.16	0.12	0.29		562	5.1	0.037	0.002	0.04	
VB3	10.1	7.0	5.4	4.7	19	23	22	21	0.156	0.116	5.0	9
VB4	49	44	0.9	0.39	0.05	0.12	11	6.5	0.006	0.001	0.55	0.45
VB5	292	189	6.5	1.5	1.1	1.0	45	20	0.006	0.011	102	33
MH1	70	102	0.09	0.35	4.5	15	469	28	0.035	0.005	2.6	0.83
MH2	84	64	0.23	0.61	0.34	1.2	241	32	0.193	0.050	3.6	1.3
MH3	73	81	0.12	0.77	2.0	3.4	286	13	0.051	0.005	2.0	1.3
MH4	85	77	0.18	0.17	1.6	2.1	120	46	0.200	0.169	11	5
OG2	85	53	0.32	18	0.28	1.7	504	84	0.011	0.002	19	0.61
OG3	44	21	4.1	2.9	4.3	5.3	86	34	0.010	0.002	40	9
OG5	34	20	1.4	12	0.19		1030	221	0.016	0.000	13	0.78
OG6	70	47	1.4	7.0	0.65	0.72	204	9.1	0.062	0.004	16	0.98
OG7	46	31	1.8	5.6	0.14		350	74	0.010	0.001	1.8	1.6
OG8	40	29	0.21	7.8	0.8	1.3	813	148	0.013	0.002	12	1.7
OG10	31	27	2.9	19	0.30	0.09	1013	201	0.016	0.001	8.3	0.54

[a] Data averaged over the final five sampling dates for the $+CO_2$ experiment: AQ on days 194, 244, 272, 305, and 334; VB on days 180, 230, 258, 291 and 320; MH and OG on days 204, 254, 282, 315, and 344. Data averaged over two sampling dates for the control (ctrl): AQ on days 194 and 305; VB on days 180 and 291; MH and OG on days 204 and 315. Averages do not include B data from AQ on day 194, VB on day 180, MH and OG on day 204.

aquifer under oxidizing conditions and atmospheric pressure will have an immediate impact on water chemistry by lowering pH and increasing the concentration of total dissolved solids. Our results showed that increased Al, Mn, Fe, Zn, Cd, Se, Ba, Tl, and U concentrations approached or exceeded their MCL under such conditions. Additionally, Li, Co, U, and Ba concentrations continued to rise after >300 days of exposure to CO_2, indicating that long-term laboratory experiments are important for understanding the risk of leaks from CO_2 sequestration. Moreover, we found significant fluctuations in Ca, Sr, Mn, and Ba over the course of 300+ days of analysis, which would not have been captured by an observation window of less than 50 days. For example, Ca in the Mahomet and Ogallala samples fluctuated between 200 and 400 ppm over the course of the experiment.

A 14-day batch experiment by Lu et al. (*27*) and a 30-day MSU-ZERT field injection study (*24*) also showed 1 to 2 unit pH declines and increases in Mg, Ca, Sr, Mn, Co, Zn, Cd, and Ba after exposure to CO_2. However, Rb, Fe, Ni, Cu, and U increased in our experiment but decreased in the Lu et al. study (Tables 2, and 3 and Figure 3e). This discrepancy may be explained by a stable, but slowly declining pH trend in our data (Figure 2) in contrast with a pH rebound that may have caused reprecipitation of the elements in the Lu et al. data. Aluminum and the oxyanion-forming trace metals (e.g., As, Se, Sb, Mo, V, and Cr) decreased in our study and in the Lu et al. batch experiment but increased at the MSU-ZERT site, consistent with the behavior of oxyanion-forming metals, which are immobilized in moderately acidic, oxidizing aqueous systems (*34, 24, 27*). The coupling of CO_2 plume modeling with laboratory experiments under a range of redox conditions should provide a robust tool for predicting the areal extent and geochemical impact of leakage (*20*).

Based on our results, the relative severity of the impact of leaks on overlying drinking-water aquifers should be considered in the selection of CO_2 sequestration sites. In the event of a CO_2 leak, Fe and Mn concentrations are likely to increase, whereas the response of other potentially harmful metals will be more varied. One primary selection criteria should be metal availability. For instance, U concentrations were higher in the Ogallala experiments relative to all aquifers sampled (Table 4). The amount of carbonate available for buffering of pH in shallow freshwater aquifers is another important factor; the highest concentrations of Al, Cr, Co, Ni, Zn, As, and Se for example were produced from our most-carbonate limited, and lowest pH, samples in our experiments. In addition to acidity, the redox state of the freshwater aquifer is also important for predicting the behavior of some elements such as U, which can be released under oxidized conditions as shown here. In our carbonate-rich samples (Mahomet and Ogallala), concentrations of As dropped after CO_2 addition. However, Apps et al. showed that under reducing conditions, solid phase As can provide a contamination source for more than 100 years (*25*).

Given the potential impacts of CO_2 leaks, chemical signatures in affected waters also provide an opportunity for early detection of such leaks. In the presence of CO_2, the elements Mn, Fe, and Ca all increased by at least an order of magnitude above control experiment concentrations within 100 days. Therefore, all three elements should be monitored, along with pH, as geochemical markers of CO_2 leaks. Dissolved inorganic carbon and alkalinity are also responsive and stable indicators of a leak (*24, 26*). Our results also show that the chemical impact of a CO_2 leak may differ within the same aquifer because of interaquifer mineralogical heterogeneities. For example, wide variations in Virginia Beach experimental pH and the behavior of Co and Ni, two elements which can be mobilized as a result of desorption from Fe and Mn oxyhydroxides (*35, 36*), suggest a heterogeneous lithology (Figure 2). Co/Ni values were similar among all Mahomet groundwater experiments but varied among the Virginia Beach samples (Figure 4). Therefore, groundwater produced from lithologically different strata in aquifers above geosequestration sites should be regularly monitored to increase the probability of an advanced detection of CO_2 leaks. Such changes may be detectable long before direct changes in CO_2 are observed, if at all.

Acknowledgments

We thank C. W. Cook and G. Dwyer for assistance with the laboratory incubations and analyses on the ICP-MS, A. Boudreau for use of the microprobe, and D. Vinson, M. Chandel, S. Osborn, A. Vengosh, B. Dressel (DOE NETL), and anonymous reviewers for helpful feedback on this manu-

script. We also thank the USGS and the people who helped us obtain sediment samples, including P. McMahon, J. J. Smith, A. Stumpf, T. S. Bruce, T. Beach, G. Harlow, and D. W. Bolton. Our research was funded by the Department of Energy through the National Energy Technology Laboratory (DE-FE0002197) and by Duke University's Center on Global Change. This report was prepared as an account of work sponsored by an agency of the U.S. Government. Neither the U.S. Government nor any agency thereof makes any warranty, express or implied, or assumes any legal liability or responsibility for the accuracy, completeness, or usefulness of any information, apparatus, product, or process disclosed.

Note Added after ASAP Publication

There was an error in Figure 1 of the version of this paper published October 26, 2010. The correct version published October 29, 2010.

Supporting Information Available

S1. $+CO_2$ groundwater experiment data by sampling day,
S2. control groundwater experiment data by sampling day,
S3. natural groundwater composition,
S4. whole rock aquifer composition,
S5. geological setting of aquifer samples,
S6. map view of Aquia, Virginia Beach, Mahomet, and Ogallala aquifers with sample locations. This material is available free of charge via the Internet at http://pubs.acs.org.

Literature Cited

(1) *Carbon Dioxide Capture and Storage*; Metz, B., Davidson, O., de Coninck, H., Loos, M., Meyer, L., Eds.; Cambridge University Press: Cambridge, 2005.
(2) Keeling, R. F.; Piper, S. C.; Bollenbacher, A. F.; Walker, J. S. *Atmospheric CO_2 records from sites in the SIO air sampling network. Trends: A Compendium of Data on Global Change*; U.S. Department of Energy: Oak Ridge, TN, 2008.
(3) Newmark, R. L.; Friedmann, S. J.; Carroll, S. A. Water Challenges for Geologic Carbon Capture and Sequestration. *Environ. Manage.* **2010**, *45* (4), 651–661.
(4) Wilson, E. J.; Friedmann, S. J.; Pollak, M. F. Research for Deployment: Incorporating Risk, Regulation, and Liability for Carbon Capture and Sequestration. *Environ. Sci. Technol.* **2007**, *41* (17), 5945–5952.
(5) Eccles, J. K.; Pratson, L.; Newell, R. G.; Jackson, R. B. Physical and Economic Potential of Geological CO_2 Storage in Saline Aquifers. *Environ. Sci. Technol.* **2009**, *43*, 1962–1969.
(6) Gale, J.; Christensen, N. P.; Cutler, A.; Torp, T. A. Demonstrating the potential for geological storage of CO_2: the Sleipner and GESTCO projects. *Environ. Geosci.* **2001**, *8* (3), 160–165.
(7) Yamazaki, T.; Aso, K.; Chinju, J. Japanese potential of CO_2 sequestration in coal seams. *Appl. Energy* **2006**, *83*, 911–920.
(8) Etheridge, D.; Leuning, R.; de Vries, D.; Dodds, K.; Trudinger, C.; Allison, C.; Fraser, P.; Prata, F.; Bernardo, C.; Meyer, M.; Dunse, B.; Luhar, A. *Atmospheric monitoring and verification technologies for CO_2 storage at geosequestration sites in Australia*; CO2CRC, Report No. RPT05-0134; 2005.
(9) U.S. Department of Energy National Energy Technology Laboratory Regional Carbon Sequestration Partnerships Website. http://www.netl.doe.gov/technologies/carbon_seq/partnerships/partnerships.html (accessed June 1, 2009).
(10) Pearce, J. M.; Shepard, T. J.; Rochelle, C. A.; Kemp, S. J.; Bouch, J. E.; Wagner, D.; Nador, A.; Veto, I.; Baker, J.; Toth, G.; Lombardi, S.; Annuziatellis, A.; Beaubien, S. E.; Ciotoli, G.; Pauwels, H.; Czernichowski-Lauriol, I.; Gaus, I.; Le Nindre, Y. M.; Girard, J.-P.; Petelet-Giraud, E.; Serra, H.; le Guern-Marot, C.; Schroot, B.; Orlic, B.; Schuttenhelm, A.; Hatziyannis, G.; Spyridonos, E.; Metaxas, A.; Gale, J.; Manancourt, A.; Brune, S.; Faber, E.; Hagendorf, J.; Poggenburg, J.; Teschner, M.; Iliffe, J.; Kroos, B.; Hildenbrand, S.; Alles, S.; Heggland, R. *The Nascent Project Final Report: Natural Analogues for the Geological Storage of CO_2*; 2005.
(11) Evans, J. P.; Heath, J.; Shipton, Z. K.; Kolesar, P. T.; Dockrill, B.; Williams, A.; Kirchner, D.; Lachmar, T. E.; Nelson, S. T. Natural Leaking CO_2-charged Systems as Analogs for Geologic Sequestration Sites. Third Annual Conference on Carbon Capture and Sequestration, Alexandria, VA, 2004.
(12) Haszeldine, R. S.; Quinn, O.; England, G.; Wilkinson, M.; Shipton, Z. K.; Evans, J. P.; Heath, J.; Crossey, L.; Ballentine, C. J.; Graham, C. M. Natural Geochemical Analogues for Carbon Dioxide Storage in Deep Geological Porous Reservoirs, a United Kingdom Perspective. *Oil Gas Sci. Technol.* **2005**, *60* (1), 33–49.
(13) Gilfillan, S. M. V.; Lollar, B. S.; Holland, G.; Blagburn, D.; Stevens, S.; Schoell, M.; Cassidy, M.; Ding, Z.; Zhou, Z.; Lacrampe-Couloume, G.; Ballentine, C. J. Solubility trapping in formation water as dominant CO_2 sink in natural gas fields. *Nature* **2009**, *458*, 614–618.
(14) Benson, S. M.; Cole, D. R. CO_2 Sequestration in Deep Sedimentary Formations. *Elements* **2008**, *4* (5), 325–331.
(15) Damen, K.; Faaij, A.; Turkenburg, W. Health, Safety and Environmental Risks of Underground CO_2 Storage - Overview of Mechanisms and Current Knowledge. *Clim. Change* **2006**, *74*, 289–318.
(16) Lewicki, J. L.; Birkholzer, J.; Tsang, C.-F. Natural and industrial analogues for leakage of CO_2 from storage reservoirs: identification of features, events, and processes and lessons learned. *Environ. Geol.* **2007**, *52* (3), 457–467.
(17) Kharaka, Y. K.; Thordsen, J. J.; Hovorka, S. D.; Nance, H. S.; Cole, D. R.; Phelps, T. J.; Knauss, K. G. Potential environmental issues of CO_2 storage in deep saline aquifers: Geochemical results from the Frio-I Brine Pilot test, Texas, USA. *Appl. Geochem.* **2009**, *24* (6), 1106–1112.
(18) Hepple, R. P.; Benson, S. M. Geologic storage of carbon dioxide as a climate change mitigation strategy: performance requirements and the implications of surface seepage. *Environ. Geol.* **2005**, *47* (4), 576–585.
(19) Keating, E. H.; Fessenden, J.; Kanjorski, N.; Koning, D. J.; Pawar, R. The impact of CO_2 on shallow groundwater chemistry: observations at a natural analog site and implications for carbon sequestration. *Environ. Earth Sci.* **2010**, *60* (3), 521–536.
(20) Carroll, S.; Hao, Y.; Aines, R. Geochemical detection of carbon dioxide in dilute aquifers *Geochem. Trans.*; 2009, *10* (4).
(21) Smyth, R. C.; Hovorka, S. D.; Lu, J.; Romanak, K. D.; Partin, J. W.; Wong, C.; Yang, C. Assessing risk to fresh water resources from long term CO_2 injection-laboratory and field studies. *Energy Procedia* **2009**, *1* (1), 1957–1964.
(22) Solomon, S. Carbon Dioxide Storage: Geological Security and Environmental Issues Case Study on the Sleipner Gas field in Norway; Bellona Report; 2007.
(23) Zheng, L.; Apps, J. A.; Spycher, N.; Birkholzer, J. T.; Kharaka, Y. K.; Thordsen, J. J.; Kakouros, E.;Trautz, R. C. Transient Changes in Shallow Groundwater Chemistry During the MSU-ZERT CO_2 Injection Experiment, American Geophysical Union Fall Meeting Abstract, 2009; H12B-5.
(24) Kharaka, Y. K.; Thordsen, J. J.; Kakouros, E.; Ambats, G.; Herkelrather, W. N.; Beers, S. R.; Birkholzer, J. T.; Apps, J. A.; Spycher, N. F.; Zheng, L.; Trautz, R. C.; Rauch, H. W.; Gullickson, K. S. Changes in the chemistry of shallow groundwater related to the 2008 injection of CO_2 at the ZERT field site, Bozeman, Montana. *Environ. Earth Sci.* **2010**, *60*, 273–284.
(25) Apps, J. A.; Zheng, L.; Zhang, Y.; Xu, T.; Birkholzer, J. T. Evaluation of potential changes in groundwater quality in response to CO_2 leakage from deep geologic storage. *Transp. Porous Med.* **2010**, *82*, 215–246.
(26) Wilkin, R. T.; Digiulio, D. C. Geochemical impacts to groundwater from geologic carbon sequestration: controls on pH and inorganic carbon concentrations from reaction path and kinetic modeling. *Environ. Sci. Technol.* **2010**, *44*, 4821–4827.
(27) Lu, J.; Partin, J. W.; Hovorka, S. D.; Wong, C. Potential risks to freshwater resources as a result of leakage from CO_2 geological storage: a batch-reaction experiment. *Environ. Earth Sci.* **2010**, *60*, 335–348.
(28) U.S. Department of Energy Carbon Sequestration Atlas of the United States and Canada Online Website. http://www.netl.doe.gov/technologies/carbon_seq/refshelf/atlas/index.html (accessed June 1, 2009).
(29) U.S. Environmental Protection Agency Drinking Water Contaminants Website. http://www.epa.gov/safewater/contaminants/index.html (accessed June 1, 2009).
(30) U.S. Geological Survey. National Water-Quality Assessment (NAWQA) Program Website. http://water.usgs.gov/nawqa/index.html (accessed June 1, 2009).
(31) Meurer, W. P.; Willmore, C. C.; Boudreau, A. E. Metal redistribution during fluid exsolution and migration in the Middle Banded series of the Stillwater Complex, Montana. *Lithos* **1999**, *47*, 143–156.
(32) Bruce, T. S.; Beach, T. Virginia Beach aquifer water well drilling logs and completion reports, unpublished, 2009.

(33) Smith, B. S.; Harlow, G. E. Conceptual Hydrogeologic Framework of the Shallow Aquifer System at Virginia Beach, Virginia. U.S. Geological Survey Water-Resources Investigations Report; 2001; 01-4262.
(34) Scanlon, B. R.; Nicot, J. P.; Reedy, R. C.; Kurtzman, D.; Mukherjee, A.; Nordstrom, D. K. Elevated naturally occurring arsenic in a semiarid oxidizing system, Southern High Plains aquifer, Texas, USA. *Appl. Geochem.* **2009**, *24* (11), 2061–2071.
(35) Alloway, B. J. *Heavy Metals in Soils*, 2nd ed.; Blackie: Glasgow, U.K., 1995.
(36) Teutsch, N.; Erel, Y.; Halicz, L.; Chadwick, O. A. The influence of rainfall on metal concentration and behavior in the soil. *Geochim. Cosmochim. Acta* **1999**, *63* (21), 3499–3511.
(37) Wilson, S. D.; Roadcap, G. S.; Herzog, B. L.; Larson, D. R.; Winstanley, D. Hydrogeology and ground-water availability in southwest McLean and Tazwell counties, Part 2: aquifer modeling and final report. Illinois State Water Survey and Illinois State Geological Survey Cooperative Groundwater Report; 1998; p 19.
(38) Herzog, B. L.; Larson, D. R.; Abert, C. C.; Wilson, S. D.; Roadcap, G. S. Hydrostratigraphic Modeling of a Complex, Glacial-Drift Aquifer System for Importation into MODFLOW. *Ground Water* **2005**, *41* (1), 57–65.
(39) Weibel, C. P.; Lasemi, Z. Illinois Geological Quadrangle Map: IGQ Villa Grove-BG, Illinois State Geological Survey, 2001.
(40) Russell, R. R. Ground-Water Levels in Illinois through 1961. State of Illinois State Water Survey Report of Investigation; 1963; p 45.
(41) Henry, M. E. Petroleum geology of the Palo Duro Basin and Pedernal Uplift provinces as a basis for estimates of undiscovered hydrocarbon resources. U.S. Geological Survey Open-File Report; 1988; 87-450-U.
(42) Fogg, G. E.; Senger, R. K. Automatic Generation of Flow Nets with Conventional Ground-Water Modeling Algorithms. *Ground Water* **1985**, *23* (3), 336–344.
(43) Meng, A. A.; Harsh, J. F. Hydrogeologic framework of the Virginia Coastal Plain. U.S. Geological Survey Professional Paper; 1988; 1404-C.
(44) Harsh, J. F.; Laczniak, R. J. Conceptualization and analysis of ground-water flow system in the Coastal Plain of Virginia and adjacent parts of Maryland and North Carolina . U.S. Geological Survey Professional Paper; 1990; 1404-F.
(45) Lehman, T. Ogallala aquifer drilling notes, unpublished, 2001.

ES102235W